Transient Method for the Liquid Laminar Flow Friction Factor in Microtubes

D. Brutin, F. Topin, and L. Tadrist
Ecole Polytechnique Universitaire de Marseille—Laboratoire I.U.S.T.I., Technopôle de Château-Gombert, 13453 Marseille, France

An original method is highlighted to determine precisely the friction factor of laminar flows in capillaries. The experiments were performed at Reynolds numbers ranging from 10 to 1,000 using a transient method and a steady-state method. The results deduced from all the implemented methods are in good agreement. Nevertheless, uncertainties differ from one method to another. A set of experiments were carried out and specific processing methods were developed. Among these methods, it was found that the integral method is the most accurate one. The friction factor obtained for capillary diameters of 320 and 530 μm are slightly higher (5.5 and 4.2%) compared to the Poiseuille law.

Introduction

The development in microfluidic systems has led to a new field of research. Micropumps, microvalves, and microchannel heat sinks for electronic devices are some examples of this wide field of applications. The understanding of physical phenomena such as the pressure drop in capillaries is essential for industrial applications (such as a microheat exchanger). Few studies have been carried out on the friction factor in capillaries due to the technical difficulties of visualizing the velocity profile inside the microtubes. The authors who have investigated this field during the past ten years do not agree on the friction factor in such a confined space even for a circular geometry. If the velocity profile in such a microtube follows a parabolic law, the friction factor which results from an integration of the shear stress will give the Poiseuille law: $64/Re$ for cylinders. However, according to the literature on microtubes, the friction factor seems to be slightly higher than the Poiseuille law (See Table 1). For example, Mala and Li (1999) obtained a friction factor up to 15% higher with fused silica and stainless steel microtubes 50 μm in diameter.

Several authors have studied water flowing in rectangular geometry due to technical difficulties in realizing precisely such a small duct of a hydraulic diameter of a few microns. This shape is realizable using a milling machine numerically controlled for a duct of depth of a few microns. Then, a simple calibrated cover plate is glued on the top to close the rectangular channel. Peng et al. (1994) investigated the flow characteristics of water flowing through rectangular microchannels having hydraulic diameters of 133 to 367 μm and a cross section aspect ratio of 0.333 to 1. They conclude from their experiments that the laminar-turbulent transition occurs at much smaller Reynolds numbers than 2,000 and the transition region is found to be within a zone with smaller Reynolds numbers than for classical channels. The hydraulic diameter and the aspect ratio have a critical effect on the liquid flow and especially on the friction factor that is mainly higher than the Poiseuille law. Popescu et al. (2000) show that, for laminar flows confined in rectangular microchannels, the pressure drop is higher for ducts of a greater hydraulic diameter. Ren et al. (2001) used polar fluids with different concentrations. They found that the concentration strongly influences the pressure drop in rectangular microchannels. They assume from their results that the electroviscous effect is the major cause of the significantly higher pressure drop for pure water, which will be discussed hereafter. Xu et al. (2000) have conducted experiments in rectangular microchannels of a hydraulic diameter of 30 to 344 μm. They found results in agreement with the Poiseuille law down to 30 μm. The uncertainty of their experiments is mainly on the hydraulic diameter accuracy. The main explanation currently proposed for these higher friction factor results in microchannels is the electroviscous effect. Due to the solid electrostatic charges which exist, the liquid charges (ions) are attracted and generate a layer of liquid of special properties

Correspondence concerning this article should be addressed to D. Brutin.

Table 1. Literature on Liquid Flow Friction Factor in Microtubes: Results Compared to Ours

Ref.	Surface	Geometry	Fluid	D_H μm	Tend.	Accuracy ($\pm$)
Present study (2002)	**Fused Silica**	**Circ.**	**Tap water**	**320.7, 539.7**	**+**	**2.3%**
Ren et al. (2001)	Silicon	Rect.	Water, KCl sol.	28–80	+	NP
Popescu et al. (2000)	Polycarbonate	Rect.	Water	128–521	+	8.8%
Weilin et al. (2000)	Silicon	Trap.	Water	51–169	+	7.6%
Xu et al. (2000)	Aluminum	Rect.	Water	30–344	id.	12%
Kulinsky et al. (1999)	Silicon	Rect.	Water, Ethanol, ...	4–100	+	NP
Mala et al. (1999)	Fused Silica, Stainless steel	Circ.	Water	50–254	+	9.2%
Mala et al. (1997)	—	Rect.	Water	—	+	NP
Peng et al. (1994)	Stainless steel	Rect.	Water	133–367	+ and −	10%
Pfahler et al. (1990)	Silicon	Rect.	*n*-propanol	1.6, 3.3	id. and +	16%

Rect: Rectangular, Circ: Circular, Trap: Trapezoidal, NP: not provided.
Tend: Friction factor tendency, +: increase, −: decrease, id: identical.

called the electrical double layer: EDL (Ren et al., 2001). According to Ren et al., the thickness of these layers can reach several micrometers for distilled water and pure organic liquids. For greater channel diameter flows, the EDL effects can be, generally, safely neglected compared to the characteristic length of the channels. All authors use the steady-state method: pressure measurements for different mass-flow rates are taken for different capillary lengths; then, accordingly the difference between the two lengths is made to subtract the inlet and outlet pressure losses.

A lot of research is needed in both theoretical and experimental areas to gain a better understanding of these phenomena. Usually, the friction factor in capillaries is found to be higher than that deduced from the Poiseuille law, but many authors do not give details of either the methods or the uncertainies associated with their results. It is important to determine precisely the friction factor. To use accurate values of this factor, it is necessary to use reliable methods and procedures. According to the literature, the values of the friction factor measured in microtubes are dispersed. Several authors find their value higher than the conventional laminar theory. On the other hand, in some cases, the value is found to follow approximately the Poiseuille flow behavior, and even to be lower than this value. This dispersion can be roughly explained by some factors such as: the different fluids used and the surface roughness.

Faced with all these diverging results, we elaborate a method to determine the friction factor which avoids some of the problems listed above. To validate our method, we choose to do our study in the simplest case with circular capillaries for which the usual law is analytically known. We measure the friction factor in these cylinders of a few hundred micron in diameter even if the comparison is difficult with rectangular geometries generally investigated in the past. We carry out different methods to determine the friction factor with steady-state measurements using forced flow and transient measurement using gravitational injection. We also propose for the transient method different data processing: (a) a derivative method and (b) an integration method. In a first part of this article, the basic equations used are presented. Then, the steady-state method usually applied for such measurements (elements of the experimental set-up, procedure and results) is presented. Next, the transient method and the different data processing methods are explained. Finally, the advantages of the integration method and the results obtained are discussed.

Basic Equations

This study deals with pressure drop, mass flow, average fluid velocity, and friction factor. All these variables defined in the notation section come from the momentum equation averaged over a cross section (Eq. 2).

The experimentally measured pressure difference is the sum of: (a) the regular pressure loss along the capillary, and (b) the singular one due to the cross section changes in inlet and outlet of the capillary (Eq. 1)

$$\Delta P(t)_{\text{measured}(m)} = \Delta P(t)_{\text{regular}(r)} + \Delta P(t)_{\text{singular}(s)} \quad (1)$$

The momentum equation can be simplified through a comparison between the fluid acceleration and the gravity one. Considering experiments of more than a few seconds and low Reynolds numbers, the fluid acceleration can be safely neglected

$$-\frac{dP_r}{dz} = \varrho\left(-g + \frac{\lambda}{D_c}\frac{U_c^2(t)}{2}\right) \quad (2)$$

Two data are needed to extract the friction factor: the pressure drop and the mass-flow rate.

The singular pressure loss is modeled as in Eq. 3 considering viscous (β) and inertial (γ) contributions

$$\Delta P(t)_s = k\frac{\varrho U_c^2(t)}{2} \quad k = \frac{\beta}{Re_c} + \gamma \quad (3)$$

For the regular pressure loss, a spatial integration from the beginning to the end of the capillary is performed assuming a fully developed flow (Eq. 4)

$$\Delta P(t)_r = \int_0^{L_c} -\frac{dP}{dz}dz = \varrho L_c\left(-g + \frac{\lambda}{D_c}\frac{U_c^2(t)}{2}\right) \quad (4)$$

The total measured pressure drop (Eq. 5) is then given by the sum of Eq. 3 and Eq. 4

$$\Delta P(t)_m = \varrho L_c\left(-g + \frac{\lambda}{D_c}\frac{U_c^2(t)}{2}\right) + k\frac{\varrho U_c^2(t)}{2} \qquad (5)$$

The two terms k and λ in (Eq. 5) can be split into a viscous and an inertial contribution. The viscous one (α/Re_c and β/Re_c) dominates when the flow is laminar and the inertial one (δ and γ) when the flow is turbulent

$$\lambda = \frac{\alpha}{Re_c} + \delta \quad k = \frac{\beta}{Re_c} + \gamma \qquad (6)$$

For a laminar flow, the friction factor form is only composed of the viscous term, so $\delta = 0$. The literature (Idel'cik, 1969) gives an estimation of the viscous term for the singular pressure drop of about 27 for β and for the inertial term of 1 for γ

$$\Delta P(t)_m = -\rho L_c g + \frac{\varrho\nu}{2D_c}U_c(t)\left[\alpha\frac{L_c}{D_c} + \beta\right] = \frac{\varrho\gamma}{2}U_c^2(t) \qquad (7)$$

The value of several terms can be roughly estimated. As shown in Table 2, the smallest ratio L/D is 625 and α is expected to be 64. An order-of-magnitude calculation shows that γ (about 1) is negligible compared with β (about 27) and $\alpha L/D$ (about 40,000).

The final relation between the total pressure drop and fluid velocity is given by Eq. 8

$$\Delta P(t)_m = -\rho L_c g + \frac{\varrho\nu\alpha L_c}{2D_c^2}U_c(t) \qquad (8)$$

The friction factor is obtained from Eq. 8 using the total pressure drop and the fluid velocity obtained with different methods and data processing.

Note for further calculation that $\alpha L_c/D_c$ is also called Δ_1

$$\Delta_1 = \frac{\alpha L_c}{D_c} \qquad (9)$$

Table 2. Capillaries Lengths Used in Steady and Transient Methods 320.7 I.D. and 539.7 μm

	320.7 μm			539.7 μm	
No.	L (mm)	L/D	No.	L (mm)	L/D
1	208.0	648.58	1	546	1012
2	297.0	926.10	2	1092	2023
3	412.0	1284.69	3	1647	3052
4	498.5	1554.41	4	2206	4087
5	870.5	2714.37	5	2348	4351
6	1018	3174.31			

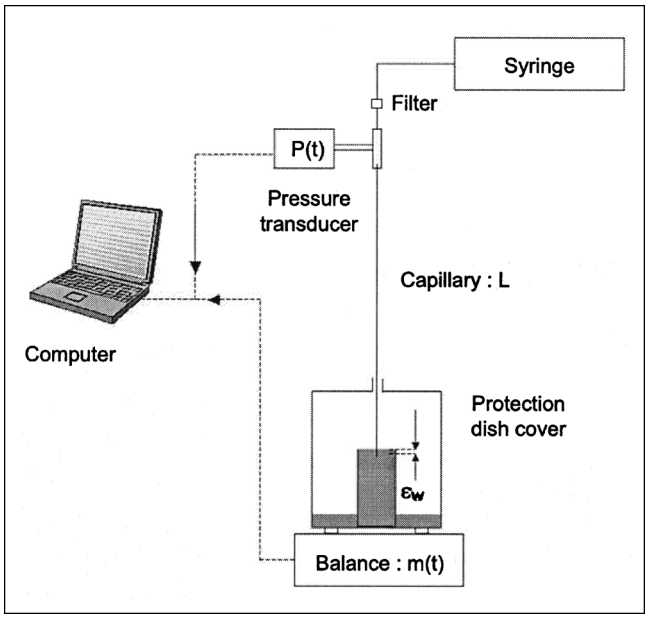

Figure 1. Experimental setup.

Steady-State Method

Experimental setup

The average fluid velocity in the capillary is deduced from the mass-flow rate measured by a weighing method. An experimental system is devised to allow an accurate measurement even for low flow rates by preventing water evaporation. In our case, the protection dish cover significantly reduces the water evaporation rate to a rate of 180 mg/h, which gives 1.8 g evaporated after a 10 h experiment; it is less than 0.5% of the maximum fluid mass weighed. Another advantage of this setup using a weighing method is that the constant pressure outlet condition can be maintained. Thus, only one pressure tap is necessary. The system is also simple to devise and not bulky for the mass-flow rate investigated (Figure 1). A K-thermocouple is placed using a T-junction before a 120 μm filter to ascertain the fluid temperature before the entrance. For each experiment, the physical parameters are calculated using the room temperature, which is constant with laboratory HVAC.

Fused silica capillaries (Restek) of 320 and 530 μm dia. commonly employed for gas chromatography are used for their smooth surface and relative low roughness. The diameter is measured to check the constructor value and determine the circularity. In fact, the circularity is needed to base our modeling on a classical parabolic velocity profile and then to compare our results with the friction factor resulting from the Poiseuille law. The internal diameter (ID) of the microtubes is measured at several locations along the microtube using an optical microscope coupled with a CCD camera. Both the diameter and circularity of a microtube cross section (Figure 2) are measured. The dimensions of the capillary are determined with an accuracy of 0.5% for about 20 cross sections. The mean measured 320.7 and 539.7 μm dia. are taken for further calculation. The observed diameter fluctuation, respectively, represents $\pm 0.33\%$ and 0.34% of the measured diameter and will constitute the uncertainties concern-

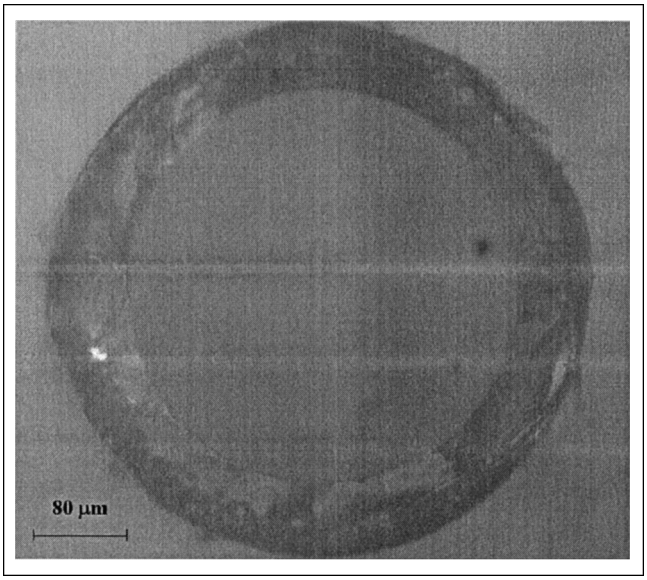

Figure 2. Typical capillary cross section ($D = 320.7\ \mu$m, $C = 1$).

ing the diameters. To measure the pressure drop due to a fully developed flow, it is necessary to ensure that the developing length is negligible in relation to the total length of the capillary. An estimation is given in a laminar flow by Eq. 10

$$\left(L_{fd}/D\right)_{lam} = 0.05 Re_D \tag{10}$$

For high Reynolds numbers reached in the capillary (1,000), the fully developed length is more than 30 times the ID of the capillary. The shortest L/D ratio is 648.6 using a 320 μm-dia. capillary which is at least 21 times as high. This is enough to allow the influence of the developing length in the pressure drop measurement to be neglected.

The microtube inlet is glued to a connector to allow a junction with the injection device and the pressure transducer. To avoid the entrance of a contaminant into the capillary, a 120 μm filter has been placed just before the capillary inlet. A length of about 10 times the hydraulic diameter is kept outside the connector to avoid any influence of the wall. The pressure is taken just at the entrance of the capillary (P_{in}) at a constant distance; whereas the outlet of the capillary (P_{out}) is under a constant height of water (ϵ_w) at a constant pressure. Different capillary lengths are obtained. The inlet and outlet conditions are made to be identical for all capillaries to allow the comparison between the different experiments. The capillary length is measured with an accuracy of 0.5 mm (Table 2).

$$P_{\text{out}} = P_{\text{atm}} + \varrho g \epsilon_w \tag{11}$$

Pressure measurements are taken just before the entrance in the microtube using a Sensym pressure sensor of sensitivity 0.57 Pa/μV. The uncertainty due to our electrical setup is 40 μV; therefore, the accuracy for the pressure signal is about 20 Pa. Simultaneously the mass which exits from the microtube is weighed at the same frequency using a Sartorius balance. The sensitivity for the range [0 g–610 g] is 8.2 mV/g with an accuracy of 76.29 μV, so about 0.01 g. The data acquisition device used is a National Instrument *PCI6033E*.

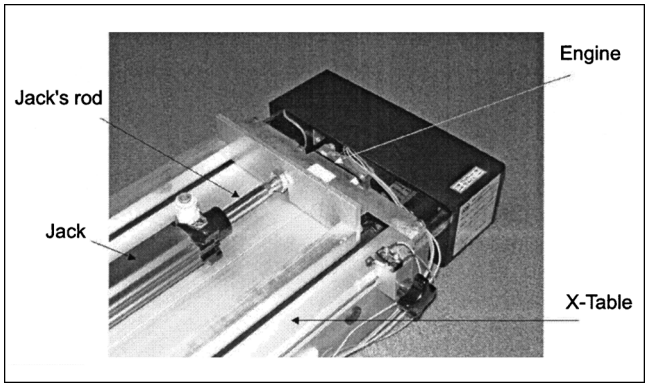

Figure 3. Hydraulic jack and X-Table photo.

The injection device used for steady measurement is a hydraulic jack (syringe) coupled with an X-Table. It allows a displacement at constant speed; therefore, a constant flow rate supplied to the capillary. The jack used has an internal diameter of 25 mm and a capacity of 0.15 L (Figure 3).

Procedure and operational method

Pressure and mass measurements are taken for all capillary lengths and mass-flow rates investigated when the steady state is reached. The data acquisition frequency chosen is usually 100 Hz. The step by step engine shifts the rod at a constant speed; the volume of water displaced is thus constant. Using rigid tubing, a constant mass-flow rate supplied to the capillary is obtained. The mass flowing through the capillary is weighed with a balance. The procedure is applied for each capillary length. Experiments are carried out to obtain the pressure drop and the mass flowing through the capillary. A procedure of evaluation of the friction factor is then applied depending on the treatment method.

For this section, Eq. 5 is used in steady state; thus, the friction term is extracted. The gravitational term, which is easily computable, is substracted. α is extracted by least-square fitting of $\Delta P_m/L_c$ as a function of U_c for all capillary lengths.

Results

The results obtained for the 320.7 μm capillaries (No. 1, No. 4, and No. 5) are shown in Figure 4. Using the pressure loss per unit length as a function of the fluid velocity for all capillary lengths, the slope, which is proportional to α, is obtained. A friction factor coefficient 10% higher than the Poiseuille law: 64 is obtained (Appendix A). So, the obtained friction factor law is

$$\lambda = \frac{70.5 \pm 5.14\%}{Re} \tag{12}$$

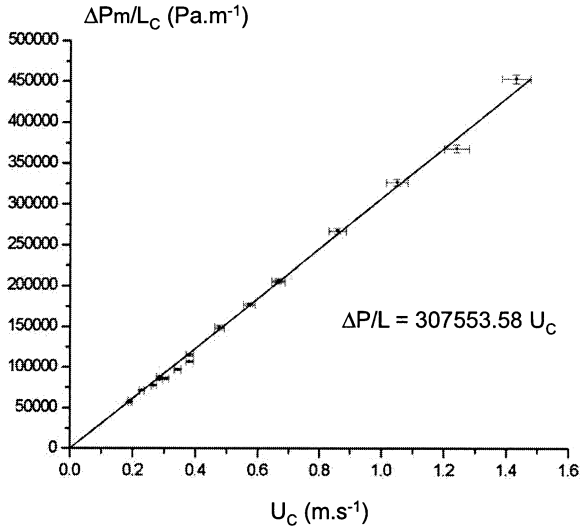

Figure 4. Pressure drop variation vs. fluid velocity for 3 capillary lengths using 320 μm-dia. capillaries [$\Delta P_m/L_c = f(U_c)$].

Transient Method

Experimental setup and procedure

The experimental setup for the transient method is composed of the data acquisition system and the capillaries previously described. The syringe is simply replaced by a 9-m-high tube of rigid calibrated tubing used as a gravitational injection device. Along a straight vertical length, it provides a constant cross section for a flowing fluid. This tube of 5.4 mm ID ± 0.02 mm has been chosen to contain a total mass of water of about 300 g. The balance is able to weigh up to 610 g and the setup on the balance weighs about 200 g. The ID of the tube must be sufficient to obtain a level of water which decreases slowly enough to neglect the acceleration pressure and the friction term in the tube ($<1\%$). The internal surface is smooth and rigid enough to have a constant cross section along the 9 m.

The tank tube is completely filled with water to have the highest pressure at the entrance of the capillary. The pressure and mass acquisition is launched while the tank water flows through the capillary at a speed which is a function of the water height. The pressure is allowed to reach 10 kPa, which corresponds to the end of the straight section; then, the acquisition is stopped. The experiment is repeated for all capillary lengths. The experiments time vary from about 1 h for a 0.2 m-long capillary to about 6 h for a 1 m-long capillary.

Identification and derivative data processing method

This method consists in using an analytical solution from the momentum equation of the pressure and mass evolution (Eq. 2). Then, by identification of the constant, it consists to derive the fitted curve to obtain the velocity evolution in the capillary. Using the two curves, pressure, and velocity, it is possible to plot the pressure loss vs. the velocity, and, thus, to extract the friction factor.

The fitting method generates errors on each constant obtained by the least-squares method. The derivative implies a multiplication and thus an increase in the error of the final results. The momentum equation is applied to the injection tube (Eq. 13). The acceleration term is negligible (<1 Pa$\cdot$m^{-1}) as is the friction term ($\simeq 10$ Pa$\cdot$m^{-1}) compared with the weight of the fluid ($\simeq 10{,}000$ Pa$\cdot$m^{-1})

$$-\frac{\partial P_t}{\partial z} = \varrho\left(\frac{\partial U_t}{\partial t} - g + \frac{\lambda}{D_t}\frac{U_t^2(t)}{2}\right) \tag{13}$$

So, the momentum equation simplified gives

$$\int_0^z \left(\frac{dP_r}{dz} = \varrho g\right) dz \quad \Delta P(t)_r = \varrho g z \tag{14}$$

$$U_t(t) = \frac{dz}{dt} = \frac{-1}{\varrho g}\frac{d\Delta P(t)_m}{dt} \tag{15}$$

Using the mass conservation equation between the injection tube and the capillary, Eq. 16 is obtained

$$U_c(t) = r^2 U_t(t) \quad r = \frac{D_t}{D_c} \tag{16}$$

It is possible to combine Eq. 8 and Eq. 15 to obtain a differential equation (Eq. 17)

$$\left(\frac{\varrho\nu\alpha L_c}{2D_c^2}\right)\frac{dU_c}{Dt} + \frac{g}{r^2 L_c}U_c = 0 \tag{17}$$

The solution of the differential equation (Eq. 17) is

$$U_c(t) = Ae^{-Ct} \tag{18}$$

The pressure solution is obtained by integrating Eq. 15, which also gives the mass evolution

$$\Delta P_m(t) = B_1(1 - e^{-Ct}) + B_2 \tag{19}$$

It is possible to calculate the pressure as a function of the velocity (from the mass equation) and thus compute Δ_1. The constants of Eq. 19 are identified by a nonlinear curve fit method processing the experimental data in a mathematical calculus software. The pressure loss vs. the fluid velocity function is plotted (Figure 5) to derive Δ_1 from each capillary using Eq. 20. The results are plotted in Figure 6, from which the slope (α) is deduced

$$\Delta P(t)_m = \Delta_1 \frac{\varrho\nu}{2D_c} U_c \tag{20}$$

The fitting method gives us a friction factor a little higher (3.1%) than the Poiseuille law (Eq. 21)

$$\lambda = \frac{66.0 \pm 5.74\%}{Re} \tag{21}$$

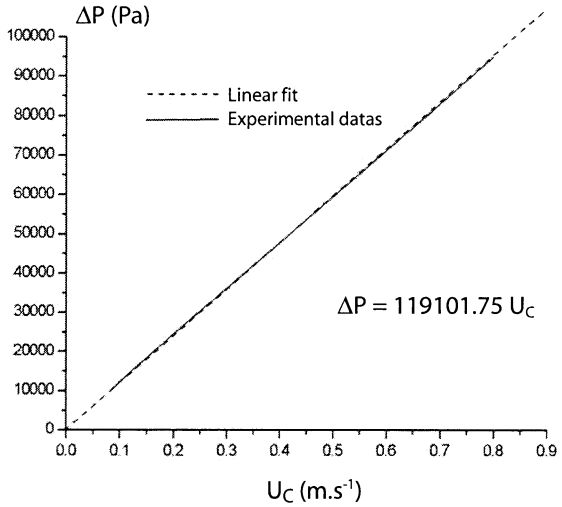

Figure 5. Pressure vs. fluid velocity using a 320 μm-dia. capillary.

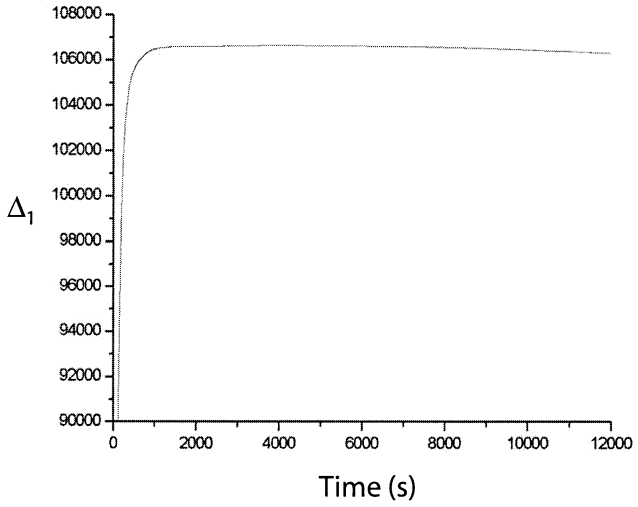

Figure 7. Δ_1 evolution as defined in Eq. 40.

Integration data processing method

This method uses the numerical integration of the experimental data. An integration in time is carried out from 0 to t to Eq. 8

$$\int_0^t \Delta P(t)_m dt = \int_0^t \left[-\rho L_c g + \frac{\varrho \nu \alpha L_c}{2D_c^2} U_c(t) \right] dt \quad (22)$$

The relation between the mass and the flow velocity (Eq. 23) allows the velocity integral to be replaced by the measured mass

$$m(t) = \int_0^t \varrho A_c U_c(t) dt \quad (23)$$

$$\int_0^t \Delta P(t)_m dt = -\rho L_c g t + \frac{2\nu\Delta_1}{\pi D_c^3} m(t) \quad (24)$$

Δ_1 is extracted from Eq. 24 and gives Eq. 25. Δ_1 is a constant, but uses functions of time as the mass weighed and the pressure integral. The Δ_1 representation should converge to an expected value (Figure 7)

$$\Delta_1 = \frac{\int_0^t \Delta P(t)_m dt + \rho L_c g t}{\frac{2\nu}{\pi D_c^3} m(t)} \quad (25)$$

Then, Δ_1 is plotted as a function of L/D; the slope obtained is the friction factor coefficients α (Figure 8).

For the 320.7 and 539.7 μm hydraulic diameter capillaries, respectively, $\alpha = 67.5 \pm 1.7\%$ and $66.7 \pm 2.3\%$ are obtained (Appendix B)

$$\lambda_{320.7} = \frac{67.5 \pm 1.7\%}{Re} \quad \lambda_{539.7} = \frac{66.7 \pm 2.3\%}{Re} \quad (26)$$

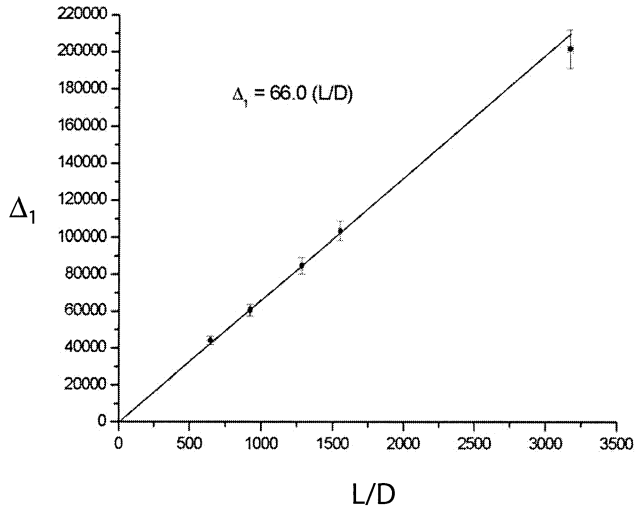

Figure 6. Δ_1 evolution vs. L/D using 320 μm-dia. capillaries for the derivative method.

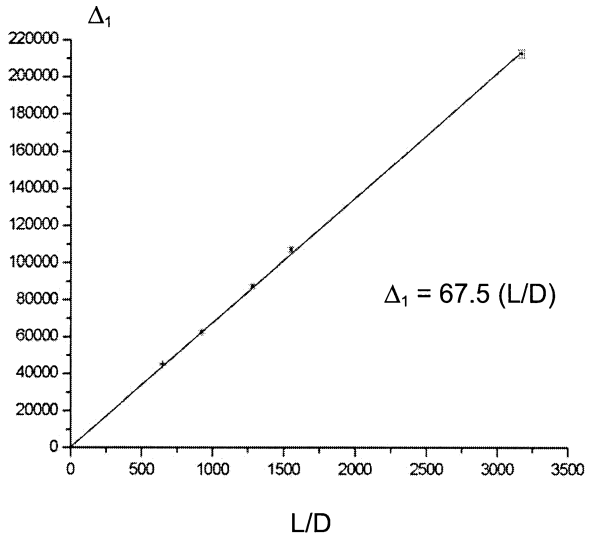

Figure 8. Δ_1 variation vs. L/D using 320 μm-dia. capillaries for the integration method.

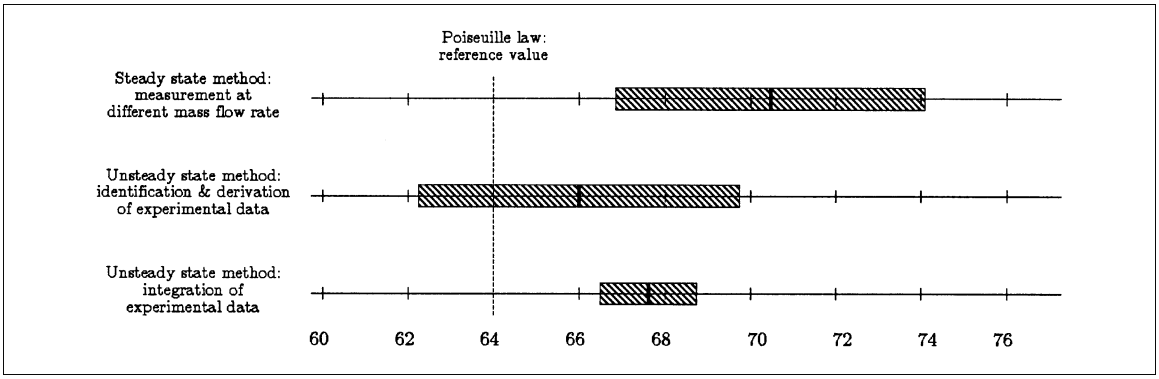

Figure 9. Comparison between the different results and uncertainty for 320 μm-dia. capillaries.

Results and Discussion

Figure 9 groups the friction factor coefficient obtained by the different methods for the 320.7 μm. The smallest uncertainty for α is obtained for the integral method with 1.7% compared with 5.1% for the steady-state method and 5.7% for the identification one. The uncertainties can vary from one method to the other, but, for each, the contribution of the hydraulic diameter is the same (Eq. 27). It is thus possible, with well calibrated hydraulic diameter capillaries, to reduce the uncertainties

$$\frac{\Delta\alpha}{\alpha} = \text{Intrinsic method error} + 4\frac{\Delta D_c}{D_c} \qquad (27)$$

Figure 9 shows the results and their uncertainties. It is thus possible to see the main tendency of a higher friction factor with a better accuracy for the integration method. All methods also agree for a friction factor ranging from $66/Re$ to $70.5/Re$ for the 320 μm-dia. capillary. The integration method has many advantages: the experimental setup is technically more straightforward. Furthermore, it is possible to have a continuous range of Reynolds numbers in only one experiment ensuring the conservation of the same friction law. Coupled with an efficient elaboration method, it is possible to obtain an accurate result ($\sim 2\%$) compared with other experimental techniques and methods found in the literature (see Table 1).

A classical method using a calibrated injection device by performing mass-flow rate and pressure loss measurements in tubes of dia. greater than 1 mm gives the Poiseuille law. Such methods applied for our capillaries give a higher friction factor than the integration method. Several assumptions could be made to explain such differences in the friction factor. The one most usually proposed is the electrical double layer (EDL) studied by Ren et al. (2001). The EDL is described to be a layer in which the fluid properties are modified due to electrostatic interaction. Inside such a layer the friction would be more significant due to a possible greater viscosity in a thin layer.

Conclusion

An original experimental setup associated with a data processing method has been elaborated to obtain precisely the friction factor of laminar flow in capillaries. This method is compared with the steady-state one (classical method) to confirm the results obtained. The results are in good agreement and the uncertainties are smaller for the proposed method. With this time-saving method, a wide range of Reynolds numbers could be investigated in only one experiment; moreover, the data processing method provides highly accurate results. The results obtained by our method gives a friction factor for a water laminar flow which is slightly higher than the Poiseuille law. The accuracy of this original method encourages us to investigate the friction factor for smaller capillaries down to 50 μm in the future. Thus, we will be able to analyze the dependency of the friction factor on the capillary diameter.

Notation

A = area, m^2
D = capillary diameter, m
F = frequency of the X-Table, Hz
g = gravitational acceleration, $m \cdot s^{-2}$
k = singular pressure loss coefficient
L = capillary length, m
m = mass, kg
P = average pressure in a cross section, Pa
r = diameter ratio (tube/capillary)
R = capillary radius, m
Re = Reynolds number
t = time, s
U = average speed in a cross section, $m \cdot s^{-1}$
z = position in the vertical axis, m

Greek letters

α = viscous coefficient (regular pressure loss)
β = viscous coefficient (singular pressure loss)
δ = inertial coefficient (regular pressure loss)
Δ = coefficient
γ = inertial coefficient (singular pressure loss)
λ = regular pressure loss coefficient
ν = kinematic viscosity, $m^2 \cdot s^{-1}$
ϱ = density, $kg \cdot m^{-3}$

Subscripts

atm = atmospheric
c = capillary
fd = fully developed
in = inlet
lam = laminar
m = measured
out = outlet
r = regular

s = singular
sy = syringe
t = tube
w = water

Literature Cited

Idel'cik, I. E., *Memento des Pertes de Charge, Eyrolles: Collection de la Direction des Etudes et Recherches d'Electricités de France*, Chapter 2, Eyrolles, Paris, France, pp. 55–89 (1969).

Kulinsky, L., Y. Wang, and M. Ferrari, "Electroviscous Effects in Microchannels," *Proc. of SPIE—The Int. Soc. for Optical Eng.*, Elsevier, 3606, 158 (1999).

Mala, G. M., D. Li, and J. D. Dale, "Heat Transfer and Fluid Flow in Microchannels," *Int. J. of Heat Mass Transfer*, **40**, 3079 (1997).

Mala, M. G., and D. Li, "Flow Characteristics of Water in Microtubes," *Int. J. of Heat and Fluid Flow*, **20**, 142 (1999).

Peng, X. F., B. X. Wang, and G. P. Peterson, "Frictional Flow Characteristics of Water Flowing through Rectangular Microchannels," *Experimental Heat Transf.*, **7**, 249 (1994).

Pfahler, J., J. Harley, H. Bau, and J. Zemel, "Liquid Transport in Micron and Submicron Channels," *Sensors and Actuators*, **1**, 431 (1990).

Popescu, S. A., A. J. Welty, D. Pfund, and D. Rector, "Pressure Drop Measurements in a Microchannel," *Fluid Mech. and Transport Phenomena*, **46**, 1496 (2000).

Ren, L., D. Li, and W. Qu, "Interfacial Electrokinetic Effects on Liquid Flow in Microchannels," *Int. J. of Heat and Mass Transfer*, **44**, 3125 (2001).

Ruo, H. C., and R. W. Hanks, "Laminar-Turbulent Transition in Ducts of Rectangular Cross Section," *Ind. Eng. Chemistry Fundamentals*, **5**, 558 (1966).

Weilin, Q., G. M. Mala, and L. Dongqing, "Pressure-Driven Water Flows in Trapezoidal Silicon Microchannels," *Int. J. of Heat Mass Transfer*, **43**, 353 (2000).

Xu, B., K. T. Ooi, N. T. Wong, and W. K. Choi, "Experimental Investigation of Flow Friction for Liquid Flow in Microchannels," *Int. Communication in Heat Mass Transfers*, **27**, 1165 (2000).

Appendix A: Experimental Uncertainty Analysis for the Steady-State Method

First, the fluid velocity is obtained using a syringe on an X-table. A frequency (F) transmitted to the X-table corresponds to a linear speed. The basic chart is obtained by measuring the linear speed of the X-table with the syringe. We obtain a relation between the syringe fluid velocity and the X-Table engine frequency with a first uncertainty

$$U_{sy} = R * F \quad R = (3.12758410^{-7} \pm 2.42\%) \tag{A1}$$

Using mass conservation, the fluid velocity in the channel is obtained

$$U_c = \frac{A_{sy}}{A_c} U_{sy} \tag{A2}$$

The microtube uncertainty is 0.35% and the syringe uncertainty is ± 10 μm for a 25 mm dia. An accuracy of $\pm 0.04\%$ for the syringe diameter is thus obtained and so an uncertainty on the fluid velocity of 3.2%.

$$\frac{\Delta U_c}{U_c} = 2\frac{\Delta D_{sy}}{D_{sy}} + 2\frac{\Delta D_c}{D_c} + \frac{\Delta R}{R} = 3.2\% \tag{A3}$$

With a pressure accuracy of 100 Pa including the offset pressure error for a minimum pressure of 10,000 Pa and a minimum capillary length of 208 mm with an accuracy of 0.5 mm, an accuracy of 1.24% is obtained on the pressure drop

$$\frac{\Delta\dfrac{\Delta P}{L}}{\dfrac{\Delta P}{L}} = \frac{\Delta(\Delta P)}{\Delta P} + \frac{\Delta L}{L} = 1.24\% \tag{A4}$$

Finally, with Eq. 32, the ultimate uncertainty of $\pm 5.14\%$ for α is obtained

$$\frac{\Delta\alpha}{\alpha} = \frac{\Delta\dfrac{\Delta P}{L}}{\dfrac{\Delta P}{L}} + \frac{\Delta U_c}{U_c} + 2\frac{\Delta D_c}{D_c} = 5.14\% \tag{A5}$$

Appendix B: Experimental Uncertainty Analysis for the Transient Method

Identification and derivative method

The pressure and mass data are fitted using the analytical solution given by Eqs. 19a and 19b. To estimate the maximum uncertainty obtained with this method, the error will be considered to be maximum using Eq. B5 at $t = 0$. The error of the pressure and the velocity is obtained using the two following equations

$$\Delta P_m(t) = B_1(1 - e^{-Ct}) + B_2 \tag{B1}$$

$$U_c(t) = \frac{-D_1 C e^{-Ct}}{\rho A_c} \tag{B2}$$

The uncertainty expressions are applied for a time which maximizes the error (usually at the end of the experiment). As an example, $B_1 = -95398.54$ Pa and $\Delta B_1 = 49.12$ Pa, which gives a relative error on B_1 of 0.05%. $B_2 = 88347.58$ Pa and $\Delta B_2 = 35.60$ Pa which gives a relative error on B_2 of 0.04%. And $C = 2.07\ 10^{-4}\ s^{-1}$ and $\Delta C = 3.276\ 10^{-7}\ s^{-1}$ so a relative error on C of 0.16%.

So the pressure loss relative error is given by

$$\Delta(\Delta P_m) = B_1(1 - e^{-Ct})\left(\frac{\Delta B_1}{B_1} + t\Delta C\right) + \Delta B_2 \tag{B3}$$

$$\frac{\Delta(\Delta P_m)}{\Delta P_m} = 1.4\% \tag{B4}$$

The velocity relative error is given by

$$\Delta U_c = \left(\frac{-D_1 C e^{-Ct}}{\rho A_c}\right)\left(\frac{\Delta D_1}{D_1} + \frac{\Delta C}{C} + 2\frac{\Delta D_c}{D_c} + t\Delta C\right) \tag{B5}$$

$$\frac{\Delta U_c}{U_c} = 3.4\% \tag{B6}$$

The friction factor relative error can be evaluated and gives 5.74%

$$\frac{\Delta\alpha}{\alpha} = \frac{\Delta\Delta P_m}{\Delta P_m} + \frac{\Delta U_c}{U_c} + 2\frac{\Delta D_c}{D_c} + \frac{\Delta L_c}{L_c} = 5.74\% \tag{B7}$$

Integration method

The uncertainty of this method is based on the expression of Δ_1 which can be split into 2 parts called, respectively, $A(t)$ and $B(t)$

$$\frac{\int_0^t \Delta P(t)_m dt + \varrho L_c g t}{\frac{2\nu}{\pi D_c^3} m(t)} = A(t) + B(t) \tag{B8}$$

$$A(t) = \frac{\pi D_c^3 \int_0^t \Delta P(t)_m dt}{2\nu m(t)} \tag{B9}$$

$$B(t) = \frac{\varrho L_c \pi D_c^3 g t}{2\nu m(t)} \tag{B10}$$

$$\frac{\Delta[A(t) + B(t)]}{A(t) + B(t)} = \frac{\Delta A(t) + \Delta B(t)}{A(t) + B(t)} = 1.1\% \tag{B11}$$

$$\frac{\Delta \alpha}{\alpha} = \frac{\Delta A(t) + \Delta B(t)}{A(t) + B(t)} + \frac{\Delta L_c}{L_c} + \frac{\Delta D_c}{D_c} = 1.69\% \tag{B12}$$

So, a final error on the integration method of 1.69%.

Manuscript received Dec. 2, 2002, revision received Mar. 19, 2003, and final revision received July 17, 2003.